Brazilian Journal of Physics
ISSN: 0103-9733
luizno.bjp@gmail.com
Sociedade Brasileira de Física
Brasil

Lima, F. M. S.; Veloso, A. B.; Fonseca, A. L. A.; Nunes, O. A. C.
Limitation of Electron Mobility in Modulation-Doped In0:53Ga0:47As/InP Quantum Wells at Low Temperatures
Brazilian Journal of Physics, vol. 36, núm. 2A, junio, 2006, pp. 365-368
Sociedade Brasileira de Física
São Paulo, Brasil

Available in: http://www.redalyc.org/articulo.oa?id=46436335

- How to cite
- Complete issue
- More information about this article
- Journal's homepage in redalyc.org

Scientific Information System
Network of Scientific Journals from Latin America, the Caribbean, Spain and Portugal
Non-profit academic project, developed under the open access initiative

Limitation of Electron Mobility in Modulation-Doped $In_{0.53}Ga_{0.47}As/InP$ Quantum Wells at Low Temperatures

F. M. S. Lima, A. B. Veloso, A. L. A. Fonseca, and O. A. C. Nunes
Instituto de Física, Universidade de Brasília, P.O. Box 04455, 70919-970 Brasília-DF, Brazil

Received on 4 April, 2005

The low-temperature electron mobility is investigated here for electrons confined in modulation-doped $In_{0.53}Ga_{0.47}As/InP$ single symmetric quantum wells. The subband structure calculation is developed via variational method, both Schrödinger and Poisson equations being solved simultaneously with adequate heterointerface matching conditions. With this in hands, the main electron scattering rates are computed, namely alloy disorder, remote ionized impurity, and interface roughness. As a result, interesting interchanges in these scattering rates were found by varying the well width and the spacer width, which show that some scattering mechanisms can surpass the alloy disorder scattering rate and come to limit the electron mobility, a behavior not reported in the literature.

Keywords: Electron mobility; $In_{0.53}Ga_{0.47}As/InP$ Quantum Wells; Low-temperature

I. INTRODUCTION

The evolution of epitaxial growth techniques for III-V semiconductor heterostructures has allowed an excellent control on both composition and doping, furnishing high-quality samples with almost abrupt heterointerfaces and doping profiles, which are crucial for the fabrication of modern electronic and optoelectronic devices [1]. It is well-known that the highest electron mobility in semiconductor heterostructures has always been observed in GaAs/AlGaAs quantum heterostructures [2], but n-doped AlGaAs carrier supply layers has some inconveniences for high-speed device applications, e.g., deep levels, interface states, and gate leakage [3]. These unwanted effects have been overcome by growing heterostructures with binary compounds in the barriers, the choice of the compounds being decisive for the device performance. In this context, $In_{0.53}Ga_{0.47}As/InP$ modulation-doped quantum wells (QWs) has been a focus of interest due to the absence of strain effects (lattice-matched heterostructure) and also due to the negligible concentrations of DX centers and dislocations on InP barrier layers [4]. Indeed, as compared to $In_{0.52}Al_{0.48}As$, another important alloy that lattice-matches to $In_{0.53}Ga_{0.47}As$, the InP supply layers present a larger Γ-L separation (630 meV in comparison to 340 meV), which reduces the probability of activation of DX-like centers and also lowers the hot carriers transfer between the channel and the doped layers [5]. However, the search for high carrier mobility in InGaAs/InP heterostructures has come up against the alloy disorder (ALLOY) scattering of electrons in the InGaAs channel, which has always been considered as the main scattering mechanism.

Since electron mobility is the physical quantity that determines the speed of electronic devices and alloy disorder is an important scattering mechanism in $In_{0.53}Ga_{0.47}As/InP$ modulation-doped QWs, we decided to investigate here in this work the possibility of other scattering mechanisms limit the mobility in such heterostructure. We considered interface roughness (IR) scattering, due to its importance in the dominance of electron mobility in thin GaAs/AlGaAs QWs [6,7], and remote ionized impurity (II) scattering, since it limits the mobility in modulation-doped QW samples with thin enough spacer layers.

II. MODEL

As convenient approximations to the subband structure calculation in $In_{0.53}Ga_{0.47}As/InP$ lattice-matched QWs we have taken into account the effective mass approximation, with Γ electrons moving in an isotropic, parabolic conduction band (CB). We consider a single symmetric QW, i.e., an $In_{0.53}Ga_{0.47}As$ channel sandwiched by InP barrier layers. The QW channel has width L and the InP barriers are doped with donors, except in the undoped spacer layers, whose width is L_S, which are essential for obtaining high-mobility in doped heterostructures [8]. The band-offset at the CB is V_0 and the doping concentration is N_D, the donor binding energy being E_D (see Ref. [9]). Since both the electron effective mass $m^*(z)$ and the dielectric constant $\varepsilon(z)$ change along the growth direction (z-axis) special forms for the Hamiltonian and the Poisson equation should be considered [9]. In this way, the coupled Schrödinger and Poisson equations read, respectively,

$$\left[-\frac{\hbar^2}{2}\frac{\partial}{\partial z}\frac{1}{m^*(z)}\frac{\partial}{\partial z}+V(z)\right]\chi_j(z)=E_j\chi_j(z) \qquad (1)$$

and

$$\frac{\partial}{\partial z}\varepsilon(z)\frac{\partial}{\partial z}V_H(z)=\frac{e^2}{\varepsilon_0}\left[N_D^+(z)-N_A^-(z)-n(z)\right]. \qquad (2)$$

The potential energy in Eq. (1) is $V(z)=V_0(z)+V_H(z)$ + $V_{XC}(z)$, where $V_0(z)$ is the CB edge of the corresponding undoped heterostructure, $V_H(z)$ is the Hartree potential, and $V_{XC}(z)$ represents the exchange-correlation corrections to the Hartree potential, included here within the local-density approximation (LDA) [8-10]. Limiting ourselves to electrons in the quantum limit, i.e. occupying only the first (ground) subband, the quantum state is determined by the subband energy level E_0 and its corresponding envelope wavefunction $\chi(z)$,

besides the wavenumber k referent to the in-plane wavevector $\mathbf{k} = k_x\,\hat{i} + k_y\,\hat{j}$. The charge concentrations on the right-hand side of Eq. (2) are $N_D^+(z)$ for ionized donors, $N_A^-(z)$ for ionized acceptors, and $n(z) = N_s\,|\chi(z)|^2$ for quasi-2D electrons in the quantum limit, N_s being the electron gas sheet density. This density depends on both the absolute temperature T and the Fermi energy E_F according to (see, e.g., Ref. [11])

$$N_s = \frac{m^*}{\pi\hbar^2}\,k_B T\,\ln\left\{1+\exp\left[(E_F-E_0)/k_B T\right]\right\}. \qquad (3)$$

It is important to note that Eq. (2) was solved within the *depletion approximation* [9], the presence of ionized residual acceptors being neglected since it has only small effects on the charge transfer [12]. Taking this approximation into account, the charge conservation equation simplifies to $L_D = N_s/(2N_D)$, with L_D being the width of the depletion layer (where all impurities are treated as being ionized).

The use of Eqs. (1) and (2) requires unusual matching conditions for the derivatives of $\chi(z)$ and $V_H(z)$ [9]. Taking the centre of the well at z = 0, the heterointerfaces will be located at $z = \pm\ell$, $\ell \equiv L/2$. For the interface at $z = +\ell$ we have

$$\frac{1}{m_A^*}\left.\frac{\partial\chi}{\partial z}\right|_{\ell^-} = \frac{1}{m_B^*}\left.\frac{\partial\chi}{\partial z}\right|_{\ell^+} \qquad (4)$$

and

$$\varepsilon_A\left.\frac{\partial V_H}{\partial z}\right|_{\ell^-} = \varepsilon_B\left.\frac{\partial V_H}{\partial z}\right|_{\ell^+}. \qquad (5)$$

The index A (B) refers to the channel (barrier) material.

In seeking for a variational scheme more accurate and flexible than the previous ones [9,12-15], we included a 2*nd*-degree term in the part of the variational wavefunction for $-\ell < z < +\ell$ (i.e., into the InGaAs channel), as given by

$$\chi(z) = B\sqrt{k_w}\left(1+cz^2\right)\,\cos(k_w z). \qquad (6)$$

For the envelope wavefunction in the barrier regions we kept the usual form, namely, $A\sqrt{a}\exp\left[\pm\frac{a}{2}(z\pm\ell)\right]$, the upper (lower) signs being for $z < -\ell$ ($z > +\ell$).

Choosing the Fermi level as the zero energy reference level, the variational method follows by deriving an analytic expression to the integral corresponding to the quantum mechanical expectation value $\left\langle\hat{H}\right\rangle = \left\langle\hat{T}+V(z)\right\rangle$ in terms of the variational parameters. The minimization of $\langle H\rangle = \langle H\rangle(k_w, c; N_s)$ was obtained by solving the 3×3 non-linear system composed by Eq. (3), with E_F = 0, and the equations $\frac{\partial}{\partial k_w}\langle H\rangle = 0$ and $\frac{\partial}{\partial c}\langle H\rangle = 0$. The numerical solution was found via Broyden's method, which is an interesting alternative to Newton's method since it is less sensitive to the initial guess and spends less running time [16].

The main scattering rates for electrons confined in InGaAs/InP heterostructures at low temperatures are well-known [8,17]. With respect to phonons, for $T < 100$ K the population of optical phonons is negligible and for $T < 60$ K acoustic phonons scattering contributes little to the mobility limitation [8]. By considering the electrons in the quantum limit, higher subbands are not populated and there is no intersubband scattering. The background impurity (BI) scattering is more complex to be calculated and will not be included here, therefore our results may not be valid for samples with residual acceptor concentrations above, say, 3 x 10^{15} cm^{-3} [18], a situation that is rarely found in samples grown by modern epitaxial techniques [2]. Thus we will concentrate only on ALLOY, IR, and remote II scattering mechanisms.

Since the carrier scattering is efficiently screened by the electron gas, the screening effect was taken into account in the lines of Ref. [19]. This effect was neglected in our ALLOY scattering rate calculation because it is essentially a short-range scattering mechanism [12].

The ALLOY scattering rate was calculated following the usual model found in literature [7,8,11], namely,

$$\frac{1}{\tau_{ALLOY}} = \frac{m_A^*}{\pi\hbar^3}x(1-x)\,\Omega\overline{V}^2\int_{-\ell}^{+\ell}dz\;|\chi(z)|^4. \qquad (7)$$

Note that the alloy is into the channel in $In_xGa_{1-x}As$/InP heterostructures. The alloy scattering parameters are defined elsewhere [11].

The IR scattering rate reads

$$\frac{1}{\tau_{IR}(k)} = \frac{m_A^*\Delta^2\Lambda^2}{2\hbar^3}\left[h(\ell)\right]^2\int_0^{2\pi}d\alpha\;(1-\cos\alpha) \times\left[\frac{1}{\varepsilon(q)^2}\;\exp\left(-\frac{\Lambda^2q^2}{4}\right)\right]_{q=2k\sin\left(\frac{\alpha}{2}\right)}, \qquad (8)$$

where $h(\ell)$ is an auxiliary function defined in Ref. [11], as well as Δ and Λ. In this equation, k is the electron wavenumber and α is the scattering angle.

The remote II scattering rate is given by [11]:

$$\frac{1}{\tau_{II}(k)} = \frac{4\pi\hbar}{m_A^*a_B^{*2}}N_D\int_0^{\pi}d\alpha(1-\cos\alpha)\;F(\alpha,k), \qquad (9)$$

where a_B^* is the effective Bohr radius. The auxiliary function in the integral is:

$$F(\alpha,k) \equiv \left[q\times\varepsilon(q)\right]^{-2}\times\int dz_i\left[g_{imp}(q,z_i)\right]^2, \qquad (10)$$

where $q = 2k\sin\left(\alpha/2\right)$ (quasi-elastic scattering approximation). The integral over z_i, the impurity position covers both depletion layers and $g_{imp}(q, z_i)$ is the form factor defined in Ref. [11].

Both the IR and II scattering times depend on k and their averages were calculated within the independent scattering approximation by doing

$$\langle\tau_i(E)\rangle = \int\tau_i(E)\,E\frac{\partial f}{\partial E}dE\Big/\int E\frac{\partial f}{\partial E}dE, \qquad (11)$$

where the index i refers to each scattering process, $E = \hbar^2 k^2 / (2\,m^*)$ is the carrier kinetic energy, and $f(E)$ is the Fermi-Dirac distribution. The partial mobilities are $\mu_i = \frac{e}{m^*} \langle \tau_i \rangle$ and the total mobility μ is computed via Matthiessen's rule, i.e., $1/\mu = \sum_i 1/\mu_i$.

III. RESULTS AND DISCUSSIONS

The variational scheme described above was implemented in MAPLE V mathematical software due to its symbolic facilities. We computed the electron subband structure and mobility for a typical example of *n*-doped $In_{0.53}Ga_{0.47}As/InP$ symmetric QW [9]. The relevant parameters are: L= 100 Å, L_S= 150 Å, V_0= 264.9 meV, $N_D = 2 \times 10^{18}$ cm^{-3}, E_D = 50 meV, and T = 4.2 K. For $In_xGa_{1-x}As$ we used $m_A^*(x)$ and $\varepsilon_A(x)$ as given in Ref. [20], with x = 0.53. For the InP barriers we used m_B^* = 0.077 m_0 and ε_B = 12.35 [9]. We found $N_s = 9.62 \times 10^{11}$ cm^{-2} for the QW example identified above, in good agreement to the usual (less accurate) variational scheme, in which $N_s \cong 9.4 \times 10^{11}$ cm^{-2} [9].

The parameters related to ALLOY scattering are the $In_xGa_{1-x}As$ lattice parameter $a_0(x) = 5.65325 + 0.40515x$ (in Å) [20], which is used to compute $\Omega = a_0(x)^3 / 4$, and $\overline{V}$= 650 meV [21]. For the IR scattering we choose $\Delta = 2.5$ Å and Λ = 120 Å [22]. Taking these parameters into account, we found $\mu_{ALLOY} = 9.16 \times 10^4$ cm^2/ Vs, $\mu_{IR} = 4.55 \times 10^5$ cm^2/Vs, and $\mu_{II} = 7.51 \times 10^5$ cm^2/Vs. This furnishes a total mobility of 6.92×10^4 cm^2/Vs. According to Ramvall *et al.* [17], a BI partial mobility of 5×10^6 cm^2/Vs is expected, due to the presence of ionized residual acceptors. This is two orders of magnitude larger than μ_{ALLOY}, which allowed us to neglect this scattering mechanism.

The dependencies of the partials and total mobilities on the well width are depicted in Fig. 1, below, for a fixed spacer thickness of 150 Å. Note that, the IR partial mobility curve crosses the ALLOY curve for $L \cong 59$ Å. Note that the IR scattering dominates entirely the total mobility behavior for smaller well widths. At the crossing point, the total mobility is 3.2×10^4 cm^2/Vs. As the II curve is one order of magnitude above the ALLOY curve, it practically does not contribute to the total mobility.

The mobility dependence on the spacer thickness is depicted in Fig. 2, for a fixed well width of 100 Å. Clearly, for L_S above, say, 750 Å the IR scattering rate overcome the ALLOY one. Note that the curve for IR partial mobility decreases with L_S due to the increase of the $h(\ell)$ auxiliary function, which enhances the IR scattering rate as seen in Eq. (8). For spacer thicknesses smaller than, say, 200 Å the rapid decrease of the II partial mobility affects the total mobility, which otherwise would increase, accompanying the ALLOY curve. In this range of spacers, the II scattering increases and leads to the formation of a maximum at L_S = 155 Å, where the mobility is 6.9×10^4 cm^2/Vs.

As seen at the left of Fig. 2, the rapid decrease of the curve for II partial mobility makes it smaller than the ALLOY one for L_S below, say, 30 Å. Unfortunately, for such small values

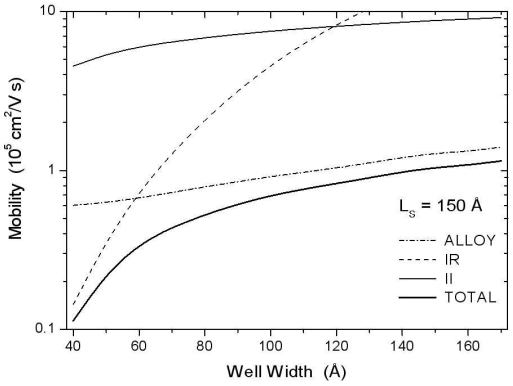

FIG. 1: Dependencies of partials and total mobilities on the well width for an InGaAs/InP symmetric QW with L_S = 150 Å. The IR and ALLOY curves cross for a well width of 59 Å. For smaller widths the IR partial mobility decreases rapid and it becomes the dominant scattering mechanism. At the crossing point, the total mobility is 3.2×10^4 cm^2/Vs.

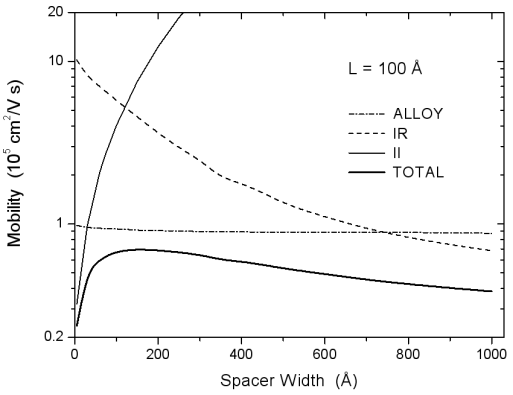

FIG. 2: Mobility dependence on the spacer thickness for a 100Å-wide InGaAs/InP symmetric QW. Note that the IR curve intercepts the ALLOY curve at $L_S \sim$750 Å. The rapid decrease of the II partial mobility for L_S below 200 Å clearly affects the total mobility, which has a maximum at L_S = 155 Å.

the charge transfer is so intense that the first subband cannot accommodate the carriers and excited subbands will be occupied. Thus, since our variational calculations are limited to the one-subband occupation regime, the results for L_S below 50 Å may be considered with caution. It would be interesting to check the mobility curves for such thin spacers by solving the problem numerically, a task that is already being developed.

IV. CONCLUSION

In this work, the mobility was calculated for quasi-2D electrons in $In_{0.53}Ga_{0.47}As$/InP single symmetric QWs. Some interesting interchanges in the low-temperature electron mobility dominance were found. To the authors knowledge, there is no indicative of such interchanges in the literature and it may be due to the belief that the ALLOY scattering always dominates the mobility in heterostructures whose channel is an alloy, as in InGaAs/InP QWs. Since these predictions should be at least qualitatively measurable, experimental results are awaited.

Acknowledgement

A.L.A.F. and O.A.C.N. wish to thank the CNPq (Brazilian agency) for the Doctor Research Grants during the course of this work. Thanks are also due to FINATEC (Brazilian agency).

[1] See, for example, V. V. Mitin, V. A. Kochelap, and M. A. Stroscio. *Quantum Heterostructures*. Cambridge Univ. Press, Cambridge MA, 1999.
[2] C. T. Foxon, J. Cryst. Growth **251**, 1 (2003).
[3] K. Radhakrishnan *et al*., J. Vac. Sci. Technol. **A18**, 713 (2000).
[4] M. J. Kelly, *Low-Dimensional Semiconductors: Materials, Physics, Technology, Devices*. Oxford U. P., New York, 1995.
[5] M. Kusters, A. Kohl, S. Brittney, T. Funke, V. Sommer, K. Heine. *InP and Related Materials*, 1993, p.473.
[6] K. Hirakawa, T. Noda, and H. Sakaki, Surf. Sci. **196**, 365 (1988).
[7] A. Gold, Z. Phys. B – Cond. Matter **74**, 53 (1989).
[8] C. Weisbuch and B. Vinter. *Quantum Semiconductor Structures*. Acad. Press, Orsay (France), 1991.
[9] F. M. S. Lima, L. C. Lapas, and P. C. Morais, Physica E **16**, 190 (2003).
[10] P. Ruden and G. H. Döhler, Phys. Rev. B **27**, 3538 (1983).
[11] F. M. S. Lima, A. L. A. Fonseca, O. A. C. Nunes, and Q. Fanyao, J. Appl. Phys. **92**, 5296 (2002).
[12] J. A. Brum and G. Bastard, Solid State Commun. **53**, 727 (1985).
[13] S. B. Ogale and A. Madhukar, J. Appl. Phys. **56**, 368 (1984).
[14] P. K. Basu and D. Raychaudhury, J. Appl. Phys. **68**, 1 (1990).
[15] K. Suresha, S. S. Kubakaddi, and B. G. Mulimani, Physica E **21**, 143 (2004).
[16] J. E. Dennis and R. B. Schnabel, *Numerical Methods for Unconstrained Optimization and Nonlinear Equations*. SIAM Class. Appl. Math. 16, Philadelphia (USA), 1996.
[17] P. Ramvall *et al*., J. Appl. Phys. **84**, 2112 (1998).
[18] F. M. S. Lima, A. L. A. Fonseca, O. A. C. Nunes, Fanyao Qu, V. N. Freire, and E. F. da Silva Jr., Physica E **17**, 322 (2003).
[19] F. M. S. Lima, Qu Fanyao, O. A. C. Nunes, and A. L. A. Fonseca, Phys. Stat. Sol. (b) **225**, 43 (2001).
[20] D. Vasileska, C. Prasad, H.H.Wieder, and D. K. Ferry, J. Appl. Phys. **93**, 3359 (2003).
[21] A. Kabasi and D. Chattopadhyay, Solid State Commun. **69**, 297 (1989).
[22] W. Wu *et al*., J. Vac. Sci. Technol. A**13**, 602 (1995).